Natural Resources Canada | Resources naturelles Canada

CANMET
MINING AND MINERAL SCIENCES LABORATORIES
LABORATOIRE DES MINES ET DES SCIENCES MINÉRALES

DIVISION REPORT / RAPPORT DIVISION

AN XPS STUDY OF BRUNSWICK MINE SULPHIDE ORE SUBJECTED TO ORE DRESSING MICROWAVE TREATMENT

Allen Pratt
Mineralogy and Metallurgical Processing

September 2001

Project: **MMSL No. 602061**
Thermal Assisted Comminution

MINING AND MINERAL SCIENCES LABORATORIES
DIVISION REPORT MMSL 01-054 (IR)

Crown Copyrights Reserved

104-05366/

EXECUTIVE SUMMARY

Complex base metal sulphide ores subjected to microwave treatment were examined for intrinsic chemical state modifications to the sulphide matrixes. The objective of the microwave treatment is to reduce the energy required for subsequent grinding and to improve the grinding efficiency. The complex sulphide ore examined was from the Brunswick mine and the major sulphide minerals were: pyrite, sphalerite, and galena. The method of analysis chosen for this investigation was X-ray photoelectron spectroscopy (XPS).

XPS was selected because it provides information on chemical bonding, atomic concentration, oxidation state and chemical speciation. Generally, XPS is regarded as a surface analysis method. However, for this study the experimental setup allowed XPS to be applied as a probe into the chemistry of the bulk material.

The XPS results presented in this study showed that the sulphide matrixes in the ore subjected to microwave treatment experienced chemical state changes. Within the samples exposed to the mildest microwave treatments, polymerized S bonds are identified. As well it appears that the atomic sites for Fe have been modified. This appears to be an indication that the microwave treatment creates (microsized) fractures within the mineral matrix. For the more vigorously treated samples, the transformation of pyrite and galena to hydroxide and oxyhydroxide species occurred.

CONTENTS

Executive Summary i

Introduction 1

Methods 2

Results and Discussion 3

Conclusions 6

References 7

Acknowledgments 8

FIGURES

Figure 1 9
Figure 2 10
Figure 3 11
Figure 4 12
Figure 5 13
Figure 6 14
Figure 7 15
Figure 8 16
Figure 9 17

APPENDIX

Appendix I 18

INTRODUCTION

Complex base metal sulphide ores subjected to microwave treatment were examined for intrinsic chemical state modifications to the sulphide matrixes. The complex sulphide ore was from the Brunswick mine and the major mineral phases present were: quartz; pyrite; sphalerite; and galena. Minor amounts of chalcopyrite, arsenopyrite, tetrahedrite, magnetite and various gangue carbonate and silicate species were also present. The mineralogy of each sample has been investigated by Laflamme (2001). (Laflamme, 2001 is included as Appendix I). The present study focuses on the pyrite, sphalerite and galena. These species were chosen because they are the most abundant sulphide minerals found in the samples examined.

Four sample lots, each consisting of several dozen rock fragments measuring up to several centimeters in size were submitted by Augustine Orumwenese (MMSL) for examination. One sample was to used as a reference material and was not exposed to any microwave treatment. The microwave treated samples were labeled A130, B310 and C530. The letter indicates a sample sequence (A to C), the first single digit is the energy (kV) and the last two digits are treatment time in minutes. All the samples exposed to microwaves were dry and immediately following the exposure period were quenched using City of Ottawa tap water. The objective of this type of microwave treatment is to reduce the energy required for subsequent grinding and to improve the grinding efficiency. Visually the sulphide grains in sample A130 have a metallic lustre; in sample B310 the sulphide grains are tarnished; and in the sample labeled C 510 the rock fragments are visibly burnt.

The method of analysis chosen for this investigation was X-ray photoelectron spectroscopy (XPS). XPS is also known as Electron Spectroscopy for Chemical Analysis or ESCA. XPS was chosen because it provides information on chemical bonding, atomic concentration, oxidation state and chemical speciation. In XPS, radiation from a soft X-ray source strikes a sample and the atoms in the bulk are excited and both core and valence band electrons are ejected with characteristic energies that are measured. Generally, XPS is regarded as a surface analysis method (Briggs and Seah, 1983). The information depth for XPS is dependent on the kinetic energy of a photoelectron and typically falls in

the 30Å to 50Å range. The XPS data can be regarded as representative of the bulk sample for the case where, below the first atom monolayer of the surface, there is little change in the matrix chemistry. However, as indicated above, the rock fragments of the submitted samples are visually altered because of the microwave treatment. Fracturing the rock fragments shows that these alterations are superficial. The XPS study was performed on fresh internal surfaces obtained by fracturing a rock fragment under vacuum. The XPS data of a surface exposed in such a manner can be considered representative of the bulk rock fragment (Briggs and Seah, 1983; Pratt et al., 1994).

METHODS

The XPS spectra were collected using a PHI-5600 equipped with an OMNI V lens system. XPS data were collected using 400 watt achromatic Al X-rays ($E_{x\text{-}ray}$ = 1486.6 eV). The energy scale of the spectrometer was calibrated to the metallic Au($4f_{7/2}$) line at 84.0 eV and to give an energy dispersion of 857.8 eV between the metallic copper 2p3/2 and 3p lines. The analyzer pass energy was 187.0 eV for the broad energy range survey scans and 11.75 eV for the narrow region energy scans. The binding energy scale of the spectra was referenced to the C1s peak from adventitious hydrocarbon (static charge referencing) and 285.0 eV was the assumed peak position. XPS information was collected from surface areas measuring near 800 x 800 μm and the vacuum in the analytical chamber was about 1.1 x 10^{-7} Pa during analysis. All spectra were deconvoluted using Shirley backgrounds, Gausian-Lorentzian peak shapes in combination with the appropriate peak fitting parameters. Details on the analysis of XPS spectra are provided in Pratt et al. (1994).

Several, randomly chosen fragments of ore from each sample lot were cut into 10 mm x 10 mm x 5 mm blocks using a high precision diamond saw. Each block was ultrasonically degreased and cleaned sequentially in EnSolv, acetone and ethanol. EnSolv is a halogenated solvent replacement for 1,1,1 - trichloroethane. Each block was then prepared for analysis by fracturing it in a high vacuum using the Conditioning Chamber for Surface Science (CCSS). The CCSS was designed and built by A. Pratt at the Mining and Mineral Sciences Laboratories (Patent applied for by NRCan). To facilitate

the analysis for these experiments, the CCSS chamber was attached via a series of UHV valves and conduits to the analytical chamber of the XPS. This allowed all manipulations of the fracture exposed surfaces to be undertaken in high to ultra high vacuum conditions.

RESULTS AND DISCUSSION

Survey Spectra

XPS survey scans collected from the fracture exposed block surfaces for each set of samples are shown in Figure 1, reference material; Figure 2, sample A130; Figure 3, sample B310; and Figure 4, sample C530. Examination of the four survey spectra shows that contributions from up to a dozen different elements can be found. These survey results show that each sample surface examined is chemically complex, and by inference mineralogically diverse. The bulk matrixes for the minerals of interest in this study are S, Zn, Pb and Fe. The element concentrations reported in this study have been calculated using a standardless method and should be regarded as semiquantitative. Using the element concentrations tabulated in each survey spectrum, a crude estimate to the relative amounts of sphalerite, galena and pyrite in each of the surface areas examined can be made. The estimate is as follows:

Reference Material - pyrite > sphalerite > galena

A130 - sphalerite > galena • pyrite

B310 - sphalerite • pyrite • galena

C530 - pyrite > sphalerite • galena

The XPS survey scans presented in Figs 1-4 collectively show element contributions from many of the various mineral phases identified by Laflamme (2001, Appendix I). In addition, to the contributions from sphalerite, pyrite, and galena. The XPS data show contributions from tetrahedrite (Sb), arsenopyrite (As), various silicates (Na, K and Ca) and various carbonates (Ca and Mg). For the data presented in Fig.1 the amount of Na calculated to be present is difficult to explain because of an apparent absence of appropriate anions. The Na contribution appears to be real and not some

spectral artifact as it is found in data collected from other fragments of fractured reference material and the contribution is found using either MgKa or AlKa radiation. Some Si and Al contributions too weak for quantitative reporting, are noted in the data. These probably originate from one of the silicate species found in the sample. The Na is probably associated with this species and the amount of Na detected might be related to the propensity for Na to migrate during microbeam chemical analysis.

High Resolution Narrow Region Spectra

S2p Spectra

S2p spectra collected from sample surfaces exposed by fracturing in the CCSS are shown in Figure 5. The spectra are all characterized by contributions near 162 eV. These contributions all arise from various forms of sulphide. An exceedingly small contribution for sulphate is observed in the S2p data for sample C530 (Fig. 5d). This is surprising considering the burnt appearance of the C530 sample.

The S2p data from the reference material show two distinct contributions, one of greater intensity near 162 eV and another of approximately half the intensity just above 163 eV. The peak separation and intensity ratio are typical of those observed for sulphide S2p3/2 and S2p1/2 spin orbit contributions (Pratt et al., 1998). The sulphide mineralogy of this sample is dominated by pyrite and sphalerite (Laflamme, 2001) and the survey scan data indicate this is the case for the area examined here as well (Figure 1, see the above section titled Survey Spectra). From this, it is expected that the S2p data would contain mainly contributions from sphalerite and pyrite. Model XPS data collected from research grade sphalerite and research grade pyrite surfaces exposed by fracture in vacuum have their respective S2p3/2 peaks at 162.5 eV (Pratt et al., 1988) and 161.8 eV (Pratt, 2001). The resolution of the data appears to be insufficient for delineation of contributions from both minerals. The data also shows a distinct tail near 161 eV. The S2p3/2 peak position for pure galena is 161.1 eV (Briggs and Seah, 1983) and the tail is interpreted to be from the sulphide in galena.

The S2p spectra collected from microwave treated samples all have remarkably similar peak shapes and positions. Unlike the reference material, there are no well defined spin orbit contributions in

the data. This may be related to differences in the mineral makeup of the samples relative to the reference sample. However, since mineral abundances differ considerably among the samples it is not unreasonable to expect some changes the in S2p spectra as well. A more likely explanation for the similar S2p spectra is that the microwave treatment imparted a similar chemical effect to the sulphide phases present. Pratt and Nesbitt (1997) observed that S2p contributions from polymerized sulphide species occur between 163 and 164 eV and that the peak position depended on the degree of polymerization. The presence of polymerized sulphide or polysulphide species in the matrix of one or more sulphide minerals following microwave treatment could impart a normalizing effect on the general appearance of any collected S2p data.

Zn2p Spectra

The Zn2p3/2 spectra collected from the 4 sample lots are shown in Fig. 6. The spectra all have similar binding energy positions near 1022 eV and similar peak shapes. This result appears to suggest that Zn is found in a similar chemical state in the samples examined. For research grade sphalerite, the Zn2p3/2 binding energy position is 1022.2 eV (Pratt, 2001) and this is similar to the binding energies reported here. Detailed examination of the data shows slight variations in the position of the 2p3/2 peak and in the spectra background at approximately 10 to 15 eV higher binding energies. The significance of these observations is unknown mainly because there is considerable confusion with regard to binding energy values for the zinc compounds commonly encountered in mineral processing. For the study of Zn ores, a systematic study detailing the diagnostic spectra for XPS analysis of model Zn bearing materials commonly encountered in metallurgical processing is recommended.

Pb4f Spectra

The Pb4f spectra collected from the 4 sample lots are shown in Fig. 7. The spectrum collected from the reference material (Fig. 7a) is characterized by two peaks of near equal intensity at 137.7 eV and 142.5 eV. These are the Pb4f7/2 and Pb4f5/2 spin orbit split peaks for galena (PbS). A slight Zn3s contribution at 140 eV is recognizable in the data. For the microwave treated sample there is a

progressive increase in the intensity from contributions at 138.3 eV and 143.2 eV. The binding energy of these contributions is similar to that reported for $Pb(OH)_2$ (Briggs and Seah, 1983; Wagner et al., 1979) and they are interpreted to result from $Pb(OH)_2$ in the material examined. $Pb(OH)_2$ is not present in the reference material and it is interpreted to have formed as a result of the microwave treatment of the ore. It is interesting to note that the mineralogical examination of these 4 samples lots found no difference in the physical appearance of galena found in the reference material or any of the microwave treated samples (Laflamme, 2001, Appendix 1).

Fe2p Spectra

The Fe2p spectra collected from the 4 sample lots are shown in Fig. 8. The spectrum collected from the reference material (Fig. 8a) is characterized by two peaks, one at 707.0 eV and another at 719.8 eV. The peak positions, shapes and relative intensities are remarkably similar to those reported for 2p3/2 (707.0 eV) and 2p1/2 (719.8 eV) photoelectron emissions from research grade pyrite surfaces exposed by fracturing in a vacuum (Mycroft et al., 1990; Nesbitt et al., 1998). There are no recognizable contributions characteristic of sphalerite (Zn,Fe)S in the Fe2p3/2 data. The Fe2p3/2 contributions for sphalerite originate from ferrous iron in a high spin electron configuration and the spectra are characterized by sharp 2p3/2 contributions at 708.9 eV and a diffuse contributions at 714.0 eV (Pratt, 2001). Ferrous iron in pyrite has a low spin configuration and the 2p3/2 photoemission is characterized by a single, sharp, well defined peak at 707.0 eV. There are most probably Fe2p contributions from sphalerite; however the intensity is exceedingly weak, and the Fe2p data collected from the reference material is interpreted to be representative of the pyrite.

Examination of the Fe2p3/2 data collected from the microwave treated samples shows a progressive increase in intensity from contributions above 707.0 eV (Fig. 8). These new contributions are most noticeable in the more intensely treated samples. The contributions are centered near 711 eV and have the binding energies and shapes characteristic of Fe(III)-oxyhydroxide (Pratt et al., 1994). These contributions are interpreted to originate from Fe(III)-oxyhydroxide species that formed within the rock matrix as a result of the microwave treatment undertaken in this study.

Comparison of the Fe2p3/2 data for the most mildly treated sample with that of the reference material (Fig. 9) shows there is an increase in the intensity of the high binding energy tail of the peak at 707.0 eV. Determination of the peak areas using accepted peak fitting routines shows that it is a 10 percent increase in intensity for the shoulder. Sphalerite in the Brunswick Mine ore contains about 8 wt% Fe in solid solution and this increase in intensity for the shoulder may be related to an increase in the amount of sphalerite in the ore. However, like the reference material, no characteristic sphalerite Fe2p3/2 contributions at 714 eV are recognized in the data. Since this feature is missing in the data it becomes difficult to accept that the intensity increase can be attributed to the amount of sphalerite present in the area of analysis. Results and interpretations presented in studies on the surface chemistry of fracture-exposed pyrite show that the shoulder is associated with iron atoms situated on, and within the first atom layer on the fracture surface (Nesbitt et al., 1998). Thus, this result appears to give some suggestion that microwave treatment followed in this study creates fractures. The fractures are most likely on a micro or even nano scale because Laflamme (2001) using secondary electron imaging could not distinguish between fractures already present in the ore and those possibly created by microwave treatment.

CONCLUSIONS

The XPS results presented in this study show that mineral matrixes well inside the rock fragments in complex base metal sulphide ore subjected to microwave treatment experience chemical state changes. Within the samples exposed to the mildest microwave treatments, polymerized S bonds are identified and it also appears that the atomic sites for Fe are modified as well. This may be an indication that the microwave treatment followed in this study creates (micro) fractures within the mineral matrixes. In the more vigorously treated samples, the transformation of sulphide species to hydroxide and oxyhydroxide species occurred. To further the understanding of mineral-microwave interactions, the examination of microwave treated research grade mineral specimens is recommended. Experiments designed to examine the effects of quenching are also recommended.

ACKNOWLEDGMENTS

The report was reviewed by Dr. R. Lastra and Dr. J. Dutrizac.

REFERENCES

Briggs D. and Seah M.P. (1983). Practical Surface Analysis by Auger and X-ray Photoelectron Spectroscopy. John Wiley & Sons, New York, 533p.

Laflamme J.H.G. (2001). Mineralogical examination of sulphide ore samples from Brunswick Mine subjected to microwave treatment, CANMET Report M-5480.

Mycroft J.R., Bancroft G.M., McIntrye N.S., Lorimer J.W. and Hill I.R. (1990). Detection of sulphur and polysulphides on electrochemically oxidized pyrite surfaces by X-ray photoelectron spectroscopy and Raman spectroscopy. Journal of Electroanalytical Chemistry, 292, 139-152.

Nesbitt H.W., Bancroft G.M., Pratt A.R. and Scaini M.J. (1998). Sulfur and iron surface states on fractured pyrite surfaces. American Mineralogist, 83, 1067-1076.

Pratt A.R., Nesbitt H.W. and Muir I.J. (1994). Generation of acids in mine waste: Oxidative leaching of pyrrhotite in dilute H_2SO_4 solutions (pH 3.0). Geochimica et Cosmochimica Acta, 58, 5147-5159.

Pratt A.R. and Nesbitt H.W. (1997). Pyrrhotite leaching in acid mixtures of HCl and H_2SO_4. American Journal of Science, 297, 807-828.

Pratt A. (2001). XPS reference spectra for sphalerite, MMSL 2001-033 (TR).

Pratt A.R., McIntyre N.S. and Splinter S.J. (1998). Deconvolution of pyrite, marcasite and arsenopyrite XPS spectra using the maximum entropy method, Surface Science 396, 266-272.

Wagner C.D., Riggs W.M., Davis L.E., Moulder J.F., and Muilenberg G.E. (1979). Handbook of X-ray Photoelectron Spectroscopy, Perkin-Elmer Corporation, Eden Prairie, Minnesota, 190p.

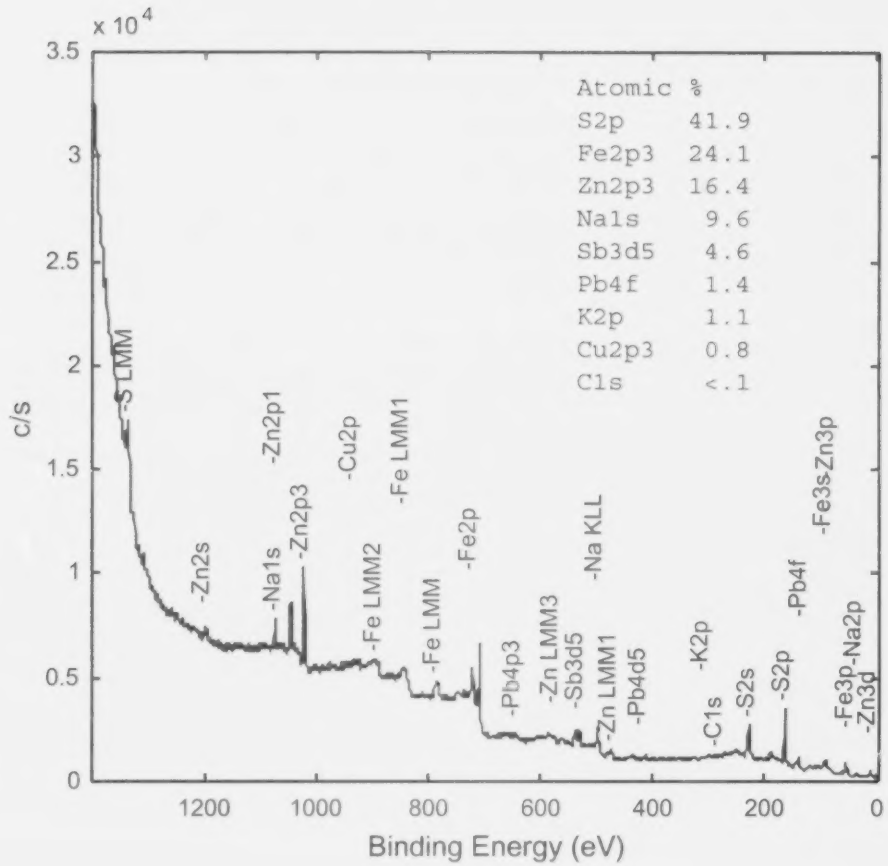

Figure 1. XPS survey scan collected from a surface of the reference Brunswick Mine sulphide. A fresh fragment surface was prepared for analysis by fracturing in a high vacuum.

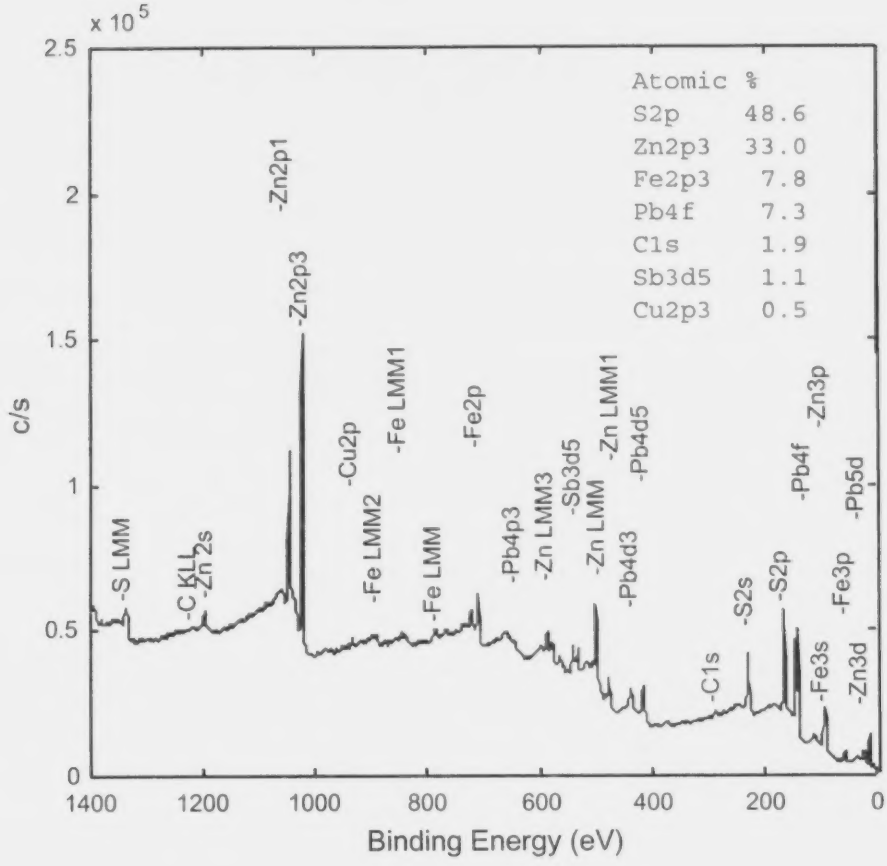

Figure 2. XPS survey scan collected from a surface of Brunswick Mine sulphide ore (sample A130) treated with microwaves and exposed by fracturing in a high vacuum.

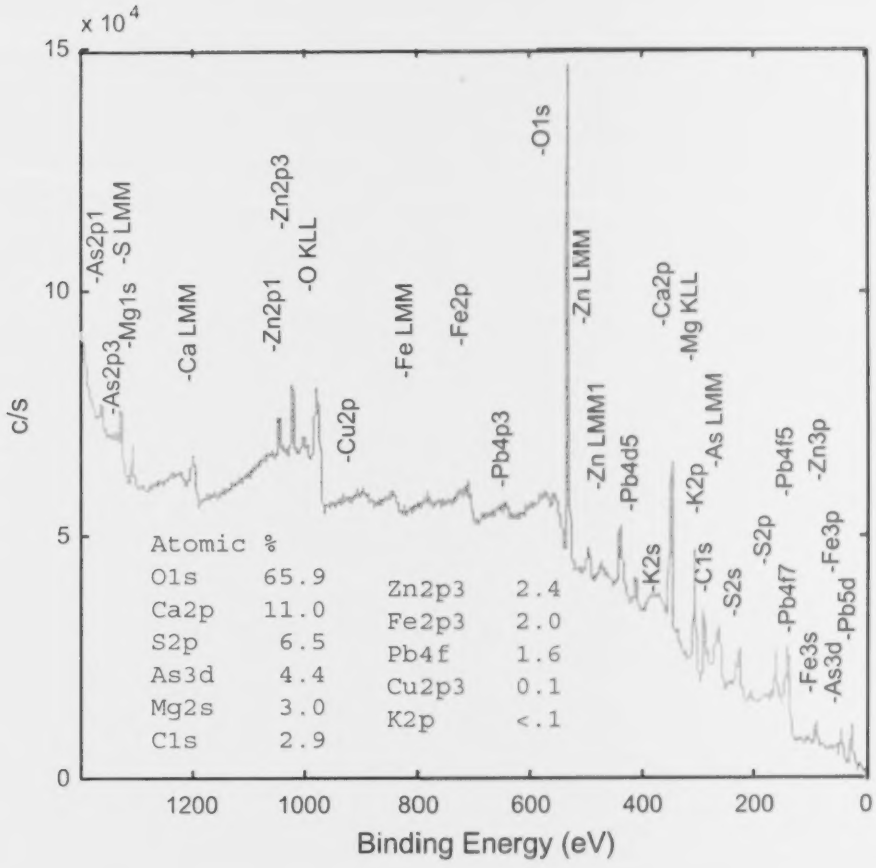

Figure 3. XPS survey scan collected from a surface of Brunswick Mine sulphide ore (sample B310) treated with microwaves and exposed by fracturing in a high vacuum.

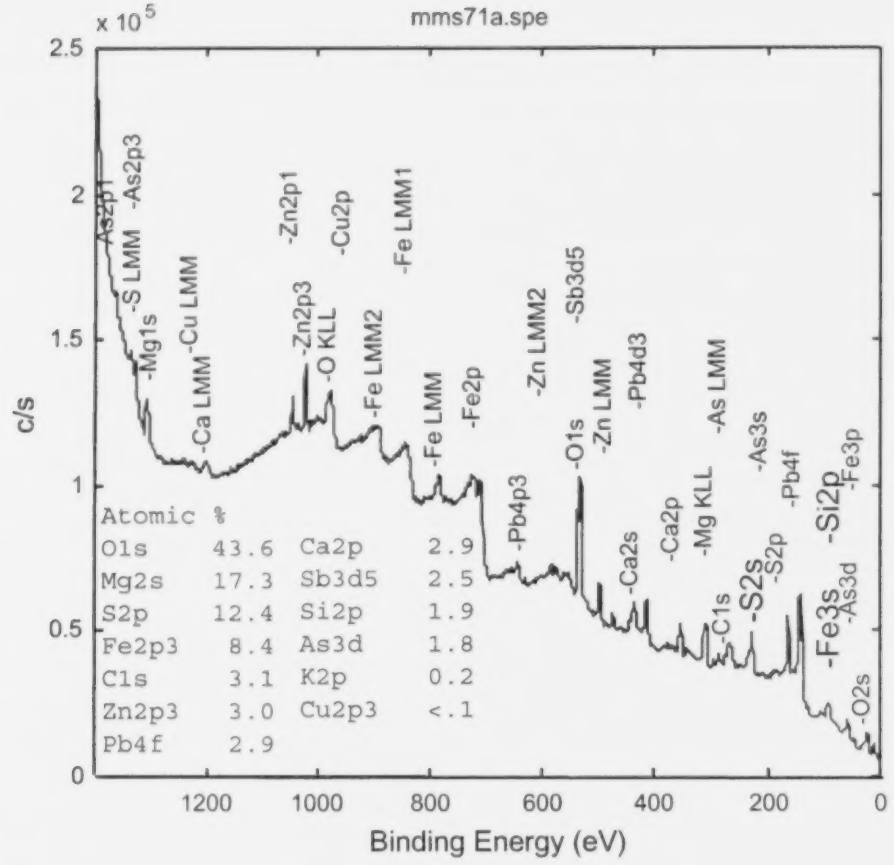

Figure 4. XPS survey scan collected from a surface of Brunswick Mine sulphide ore (sample C530) treated with microwaves and exposed by fracturing in a high vacuum.

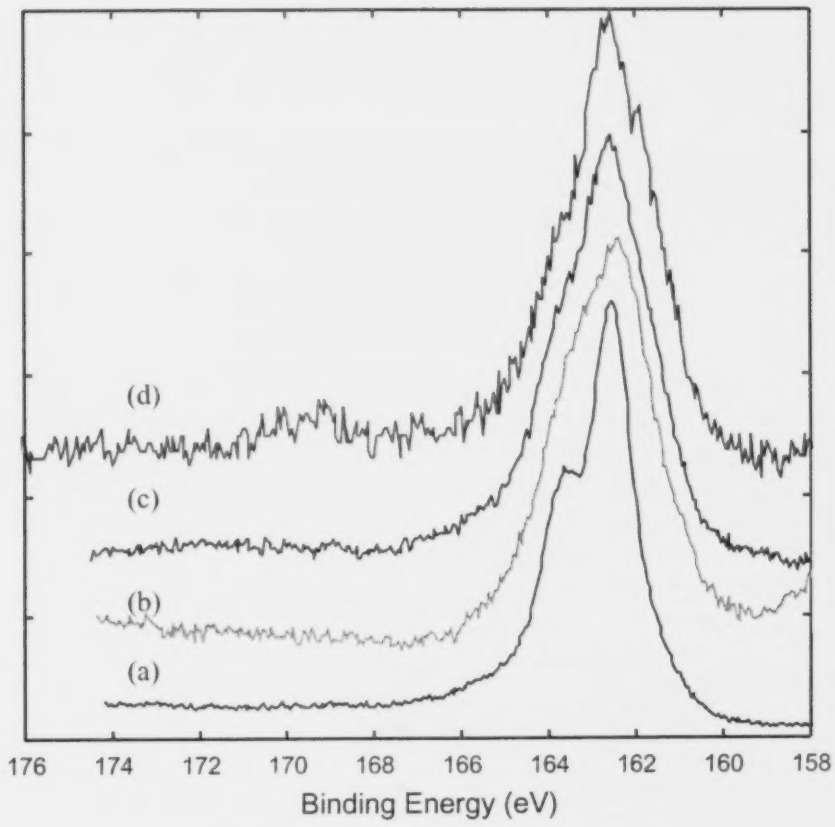

Figure 5. S2p spectra collected from surfaces exposed by fracture in a high vacuum: (a) reference sample; (b) sample A130; (c) sample B310; and (d) sample C530.

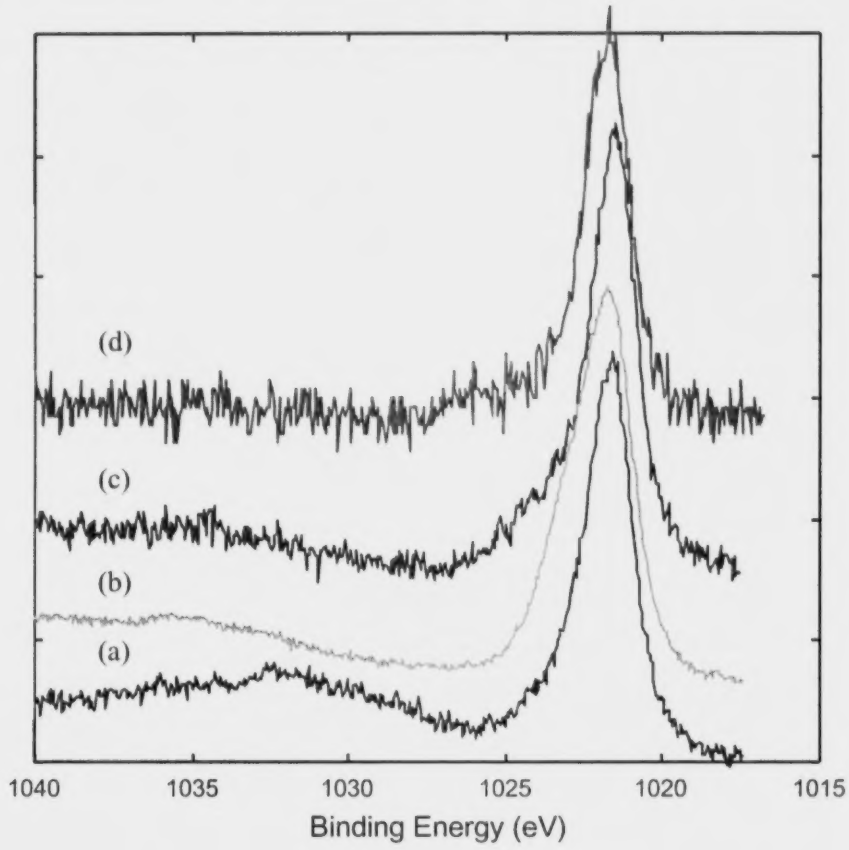

Figure 6. Zn2p3/2 spectra collected from surfaces exposed by fracture in a high vacuum: (a) reference sample; (b) sample A130; (c) sample B310; and (d) sample C530.

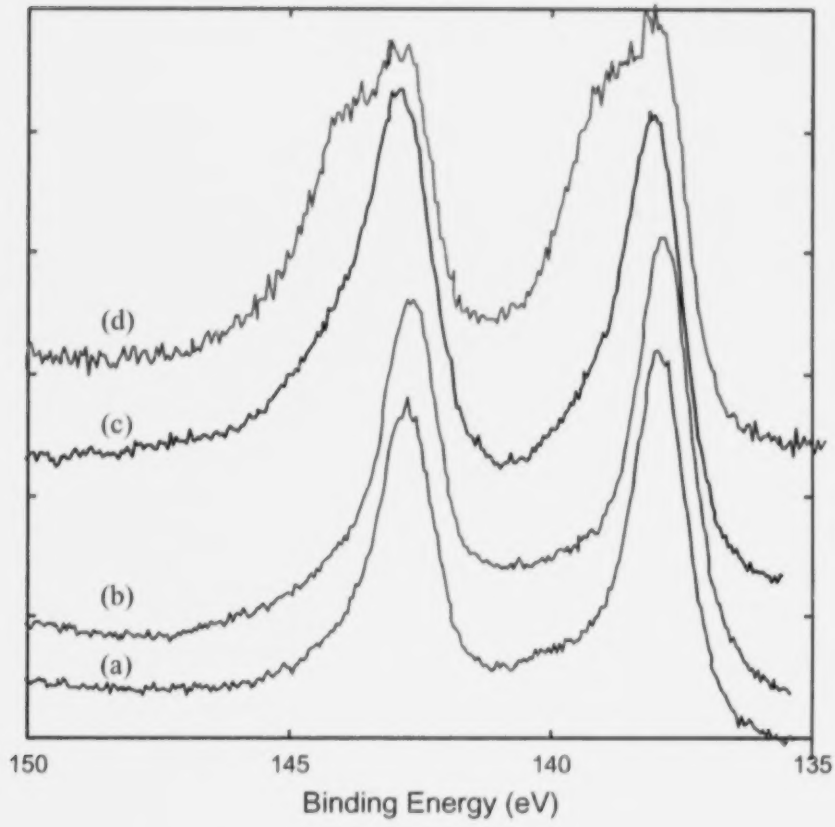

Figure 7. Pb4f spectra collected from surfaces exposed by fracture in a high vacuum: (a) reference sample; (b) sample A130; (c) sample B310; and (d) sample C530.

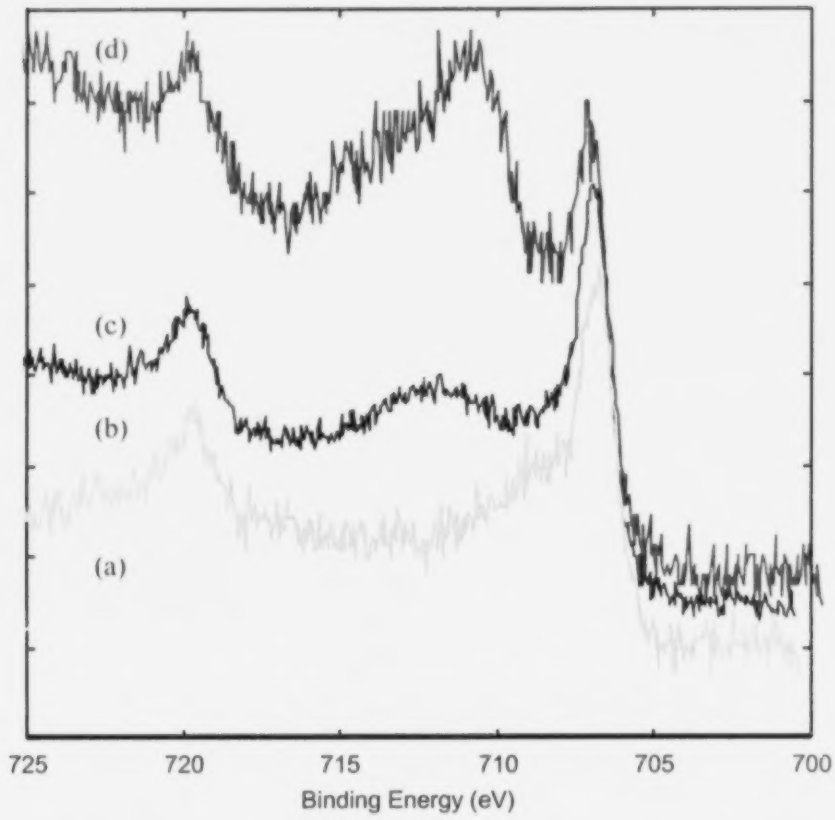

Figure 8. Fe2p spectra collected from surfaces exposed by fracture in a high vacuum: (a) reference sample; (b) sample A130; (c) sample B310; and (d) sample C530.

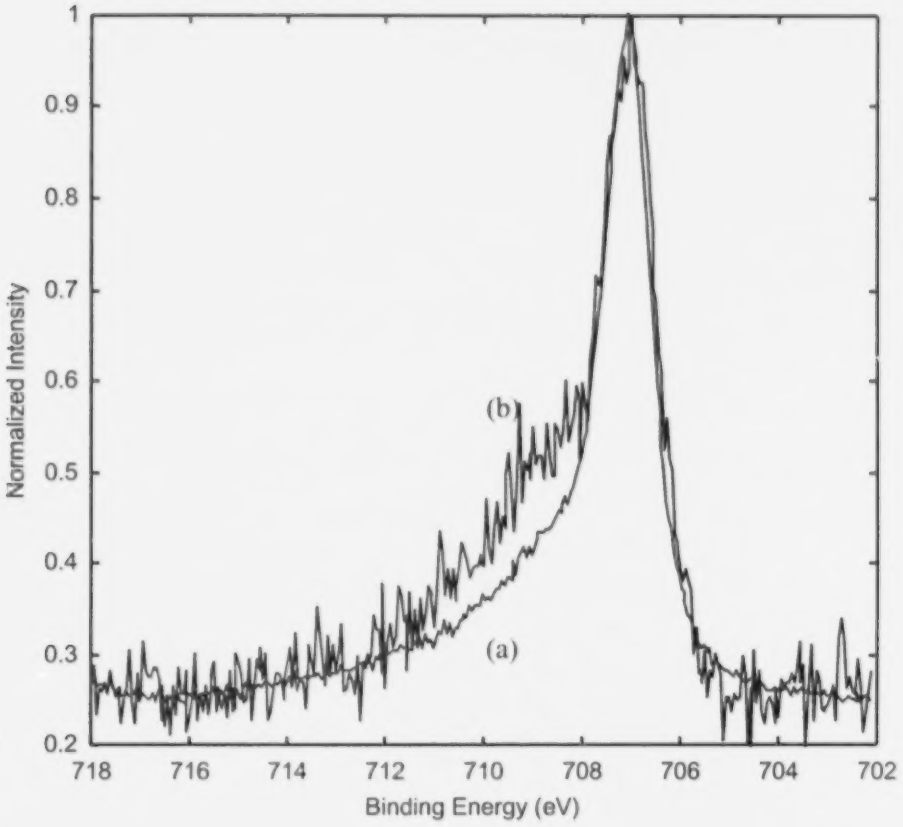

Figure 9. Fe2p3/2 spectra collected from surfaces exposed by fracture in a high vacuum: (a) reference sample; (b) sample A130. Peak intensities have been normalized and backgrounds removed.

Appendix I

A copy of the CANMET Report M-5480 by Laflamme J.H.G. (2001) entitled Mineralogical examination of sulphide ore samples from Brunswick Mine subjected to microwave treatment.

MINING AND MINERAL SCIENCES LABORATORIES

MINERALOGICAL CHARACTERIZATION GROUP

REPORT M - 5480

TITLE: Mineralogical examination of sulphide ore samples from Brunswick Mine subjected to microwave treatment.

INVESTIGATOR: J.H.G. Laflamme

PROJECT NO.: 602061

SAMPLE: The samples consist of six polished sections containing three sulphide ore samples from the Brunswick Mine, before and after being subjected to microwave treatment. The polished sections were labelled as A, B, C (before treatment), A-M, B-M , and C-M (after treatment); these were submitted on April 26, 2001 by Augustine Orumwenese (MMSL).

PURPOSE: To perform descriptive mineralogy and compare the mineralogy of the samples before and after the microwave treatment. Also to compare the relative proportions of intergranular and transgranular cracks, before and after the microwave treatment.

METHOD OF INVESTIGATION: The polished sections were first examined by optical microscopy, followed by scanning electron microscopy on a JEOL 820 electron microscope, operated at 20 kV, with a specimen current of 1 nA. Identifications were done by Energy Dispersion Spectrometry (EDS), using a Link ISIS 300 system. Digital images were acquired by both optical and scanning electron microscopy, to show distinct features.

RESULTS:

Sample A

Optical examination of the sample prior to the microwave treatment reveals a typical complex sulphide ore (Fig. 1), with pyrite as the major sulphide present, with minor to trace amounts of sphalerite, chalcopyrite, arsenopyrite, galena, Ag-bearing tetrahedrite and magnetite. Gangue minerals are mainly calcite, with lesser amounts of stilpnomelane, ankerite and apatite. The examination of the sample after the microwave treatment does not show any distinct features compared to the same sample prior to the treatment. No apparent intergranular or transgranular cracks are observed.

Signed _____ Date _____ Approved _____ Date _____
INVESTIGATOR John Dutrizac

1. _____ 2. Augustine Orumwnese 3. Section Files ORIGINATOR (2 copies)
PROJECT LEADER

4. _____

_____

PLEASE NOTE: THIS REPORT NOT TO BE REFERENCED IN PUBLICATIONS
PLEASE ACKNOWLEDGE THIS WORK IN FINAL REPORT

Sample B

Before the microwave treatment, this sample shows mainly pyrite, which is often well crystallised as shown in Figure 2. Trace amounts of sphalerite, chalcopyrite and galena are present. Gangue minerals are mainly quartz with much lesser amounts of ankerite, calcite, celsian, apatite, rutile and cassiterite. A study of the sample following the treatment reveals severe alteration of pyrite to a goethite-like phase, in parts of the sample as shown in Figure 3. As shown in the backscattered electron images (Figs. 4 and 5), cracks have developed around the pyrite grains and along their grain boundaries.

Sample C

Similar to sample A, examination of this sample before the treatment, reveals a complex sulphide ore with pyrite as the major sulphide, and minor to trace amounts of sphalerite, arsenopyrite, chalcopyrite, galena, Ag-bearing tetrahedrite and stannite (Figs. 6 and 7). A study of the sample following the microwave treatment reveals severe alteration, which is obvious even during macroscopic examination. A study by optical and scanning electron microscopy reveals a complete alteration of the pyrite to a S- and As-bearing goethite-like phase. Cracks have developed around the pyrite remnants, which also developed within the sphalerite host in some areas (Figs. 8-10).

CONCLUSION: It appears that the microwave treatment used for sample A was not sufficient to modify the sample, although the treatment was too severe for sample B where partial alteration of the pyrite was observed. The treatment was even more severe with sample C, which shows complete alteration of the pyrite, to a S- and As-bearing goethite-like phase. In both cases, cracks have developed around and along the pyrite grain boundaries.

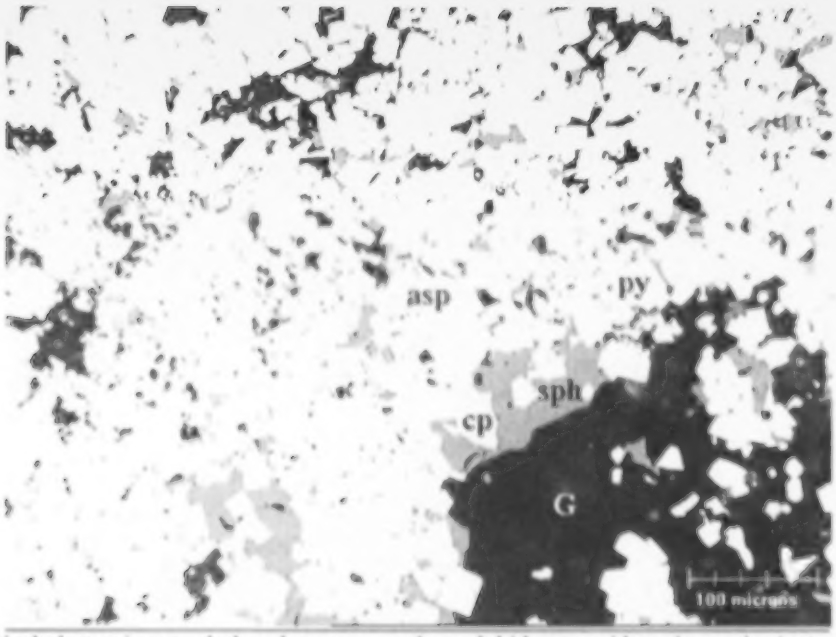

Figure 1. Optical photomicrograph that shows a complex sulphide ore, with major pyrite (py), with minor to trace amounts of sphalerite (sph), arsenopyrite (asp), chalcopyrite (cp), and gangue (mainly calcite, G); Sample A

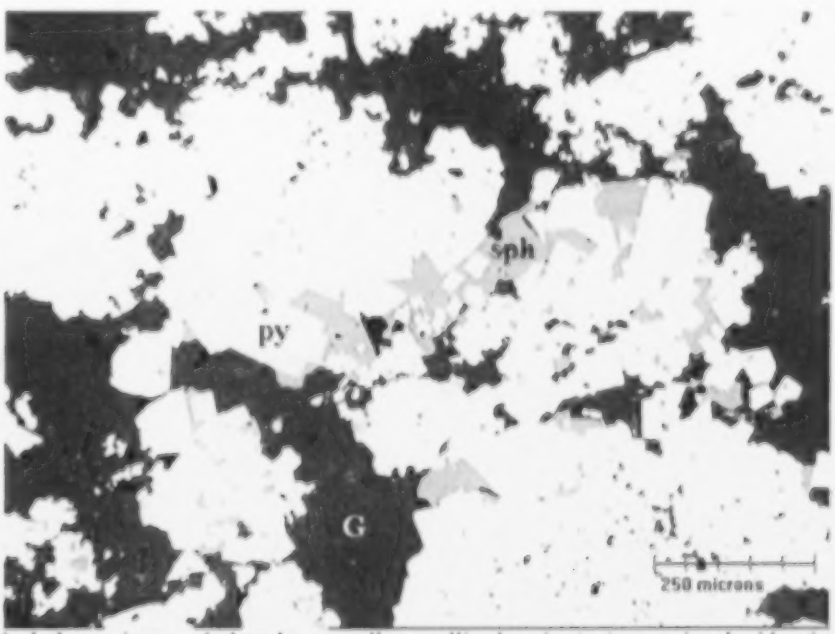

Figure 2. Optical photomicrograph that shows well crystallised pyrite (py), associated with minor sphalerite (sph) and gangue (mainly quartz, G); Sample B

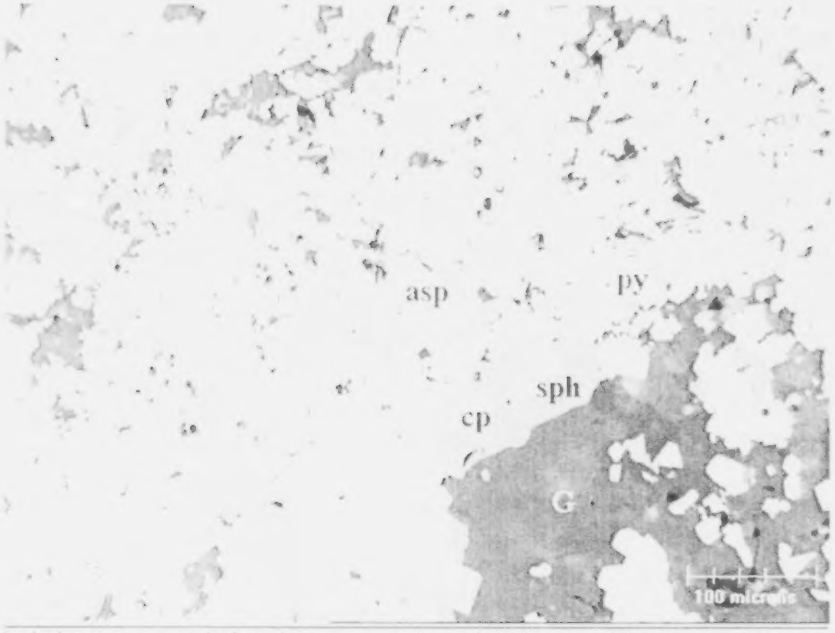

Figure 1. Optical photomicrograph that shows a complex sulphide ore, with major pyrite (py), with minor to trace amounts of sphalerite (sph), arsenopyrite (asp), chalcopyrite (cp), and gangue (mainly calcite, G). Sample A

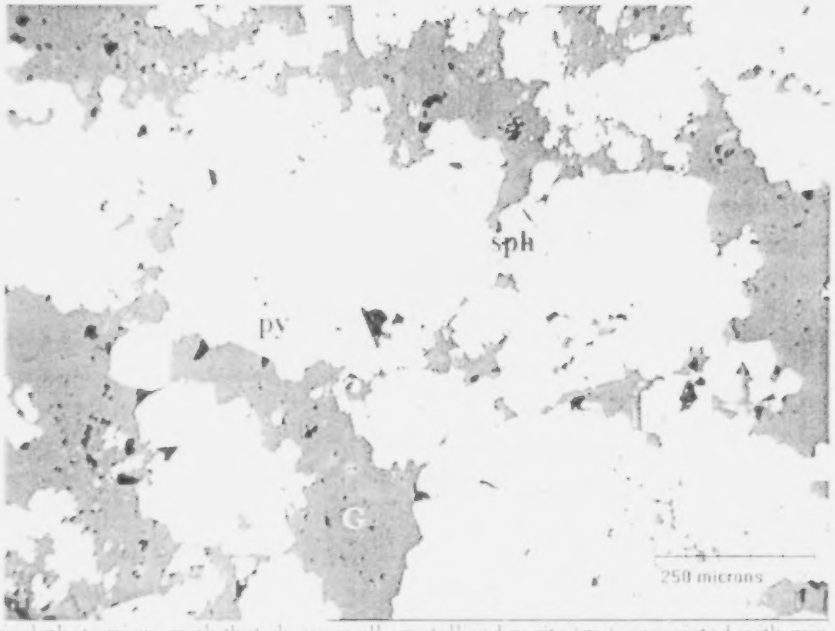

Figure 2. Optical photomicrograph that shows well crystallised pyrite (py), associated with minor sphalerite (sph) and gangue (mainly quartz, G). Sample B

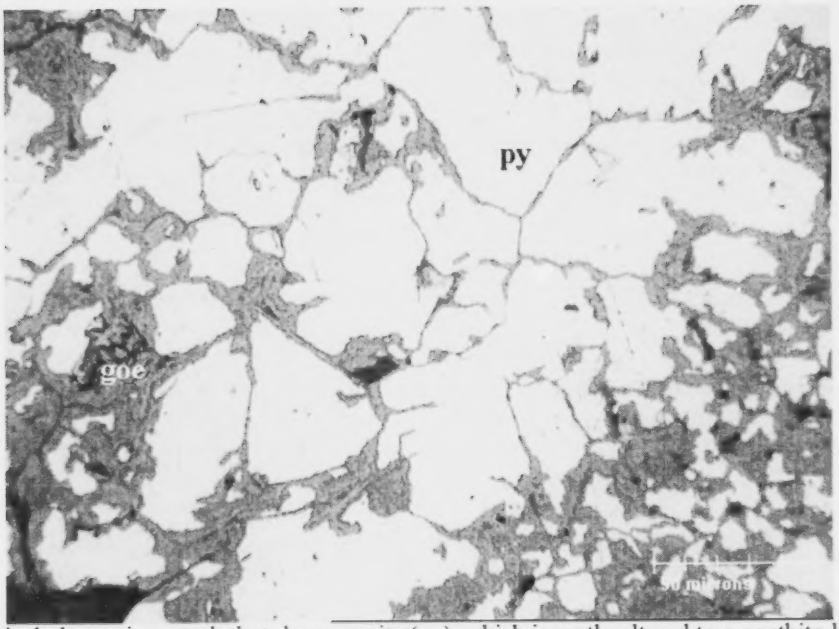

Figure 3. Optical photomicrograph that shows pyrite (py), which is partly altered to a goethite-like phase (goe) along grain boundaries; Sample B-M

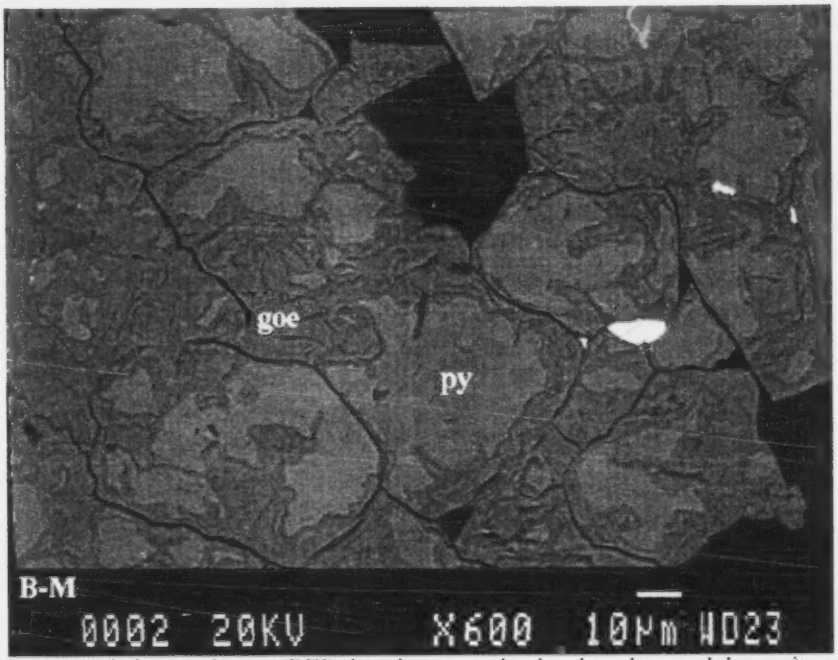

Figure 4. Backscattered electron image (BEI) that shows cracks developed around the pyrite grains (py), which are partly altered and replaced by a goethite-like phase (goe); Sample B-M

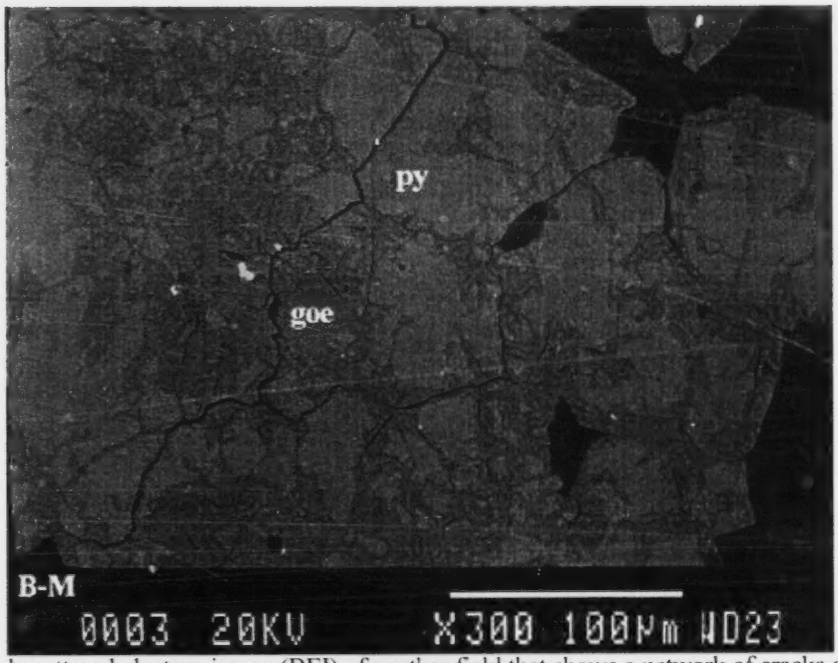

Figure 5. Backscattered electron image (BEI) of another field that shows a network of cracks developed along the pyrite (py)/goethite (goe) grain boundaries; Sample B-M

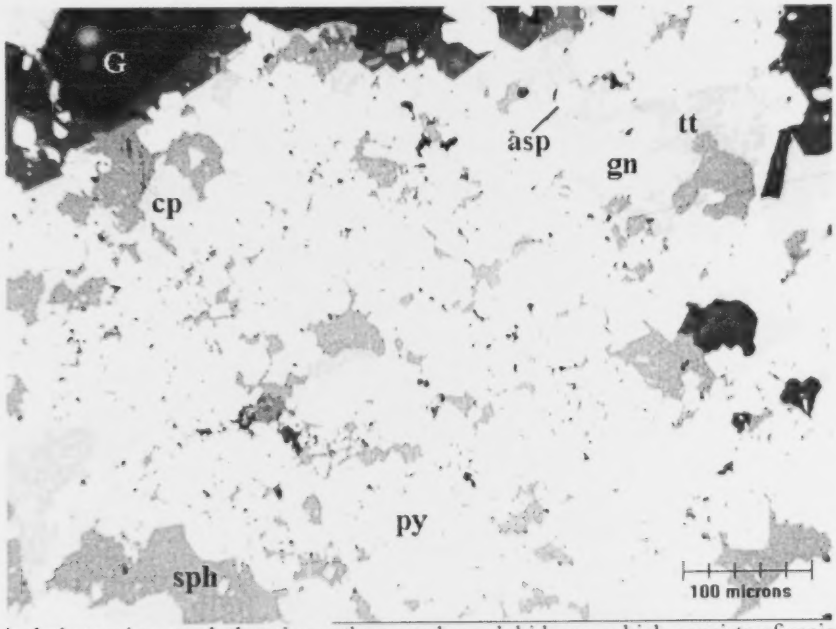

Figure 6. Optical photomicrograph that shows the complex sulphide ore which consists of major pyrite (creamish white), with minor to trace amounts of sphalerite (grey), arsenopyrite (bluish white), chalcopyrite (yellow), galena (gn), Ag-bearing tetrahedrite (tt) and gangue (mainly quartz, dark grey); Sample C

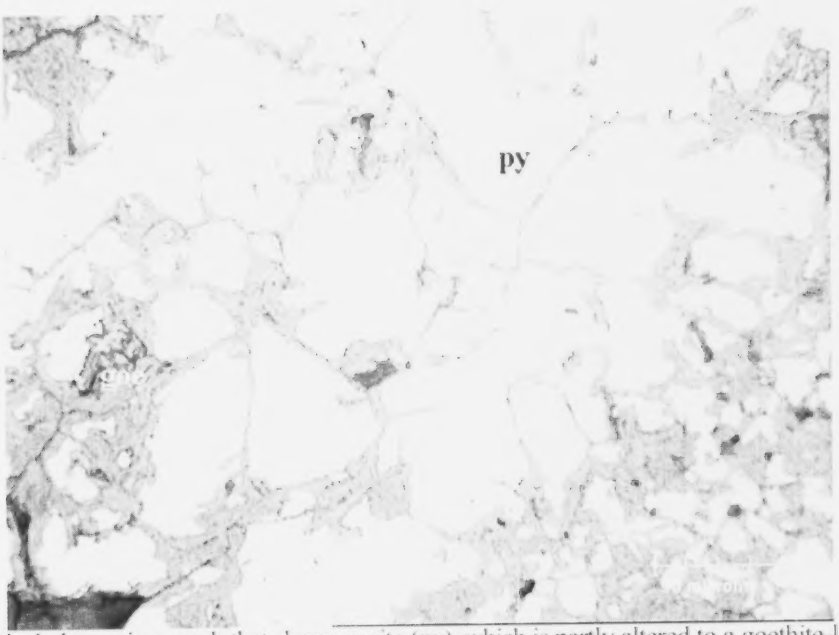

Figure 3. Optical photomicrograph that shows pyrite (py), which is partly altered to a goethite-like phase (goe) along grain boundaries; Sample B-M

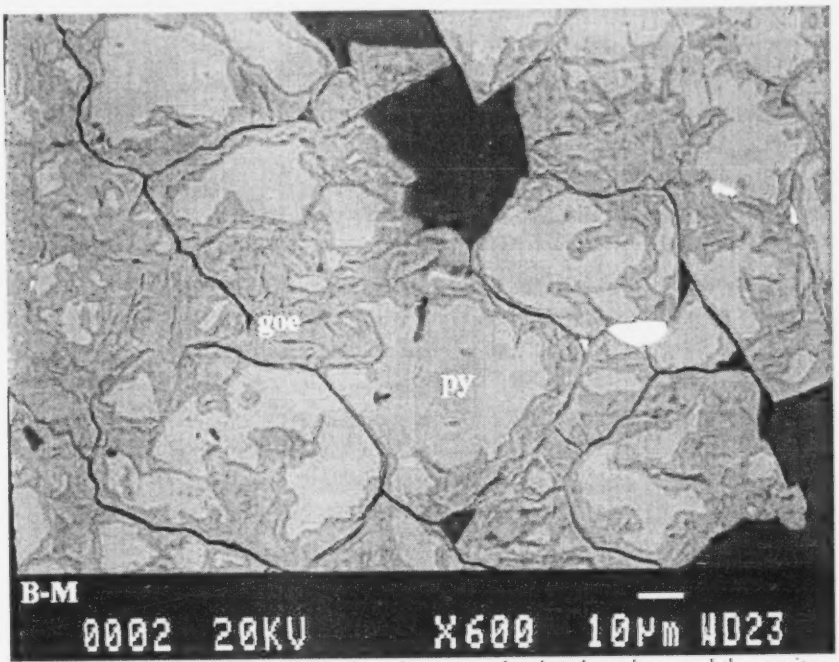

Figure 4. Backscattered electron image (BEI) that shows cracks developed around the pyrite grains (py), which are partly altered and replaced by a goethite-like phase (goe); Sample B-M

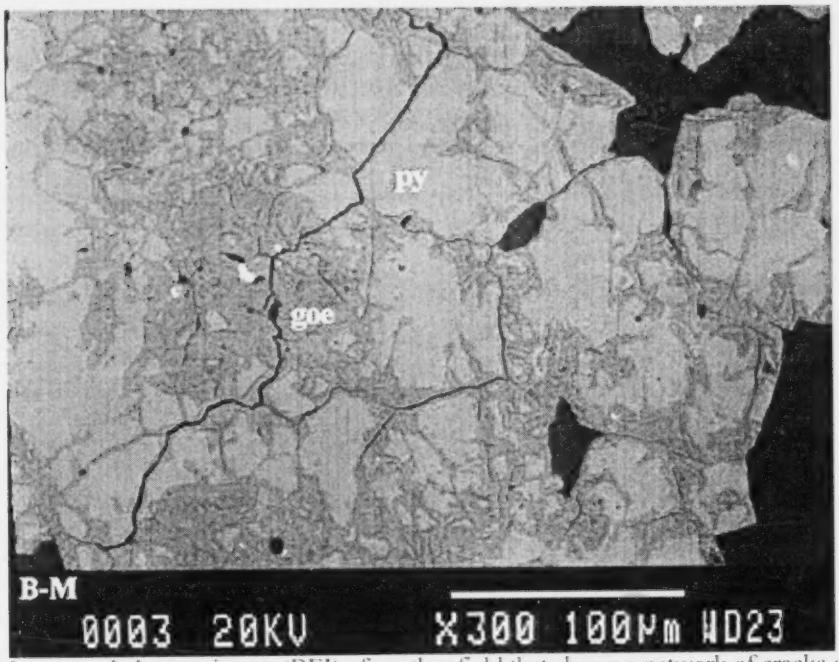

Figure 5. Backscattered electron image (BEI) of another field that shows a network of cracks developed along the pyrite (py)/goethite (goe) grain boundaries: Sample B-M

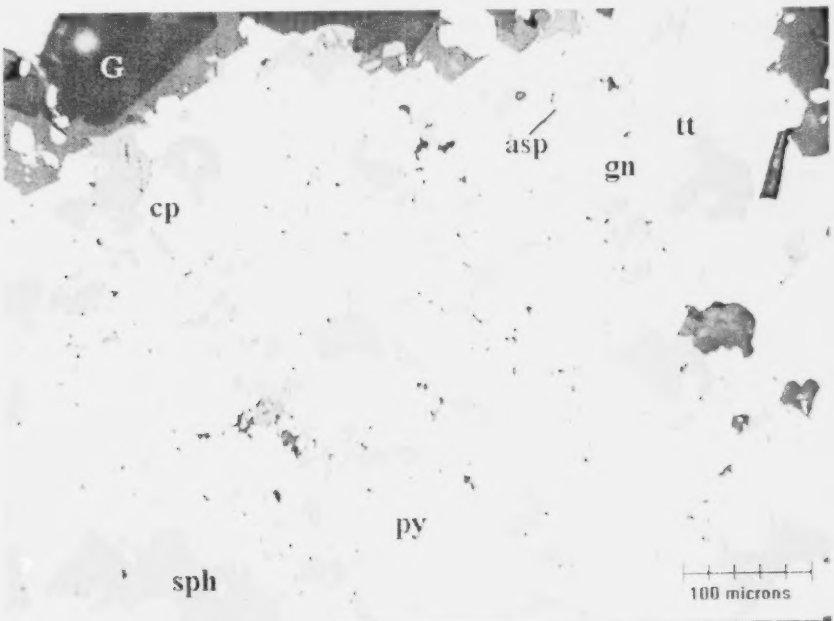

Figure 6. Optical photomicrograph that shows the complex sulphide ore which consists of major pyrite (creamish white), with minor to trace amounts of sphalerite (grey), arsenopyrite (bluish white), chalcopyrite (yellow), galena (gn), Ag-bearing tetrahedrite (tt) and gangue (mainly quartz, dark grey): Sample C

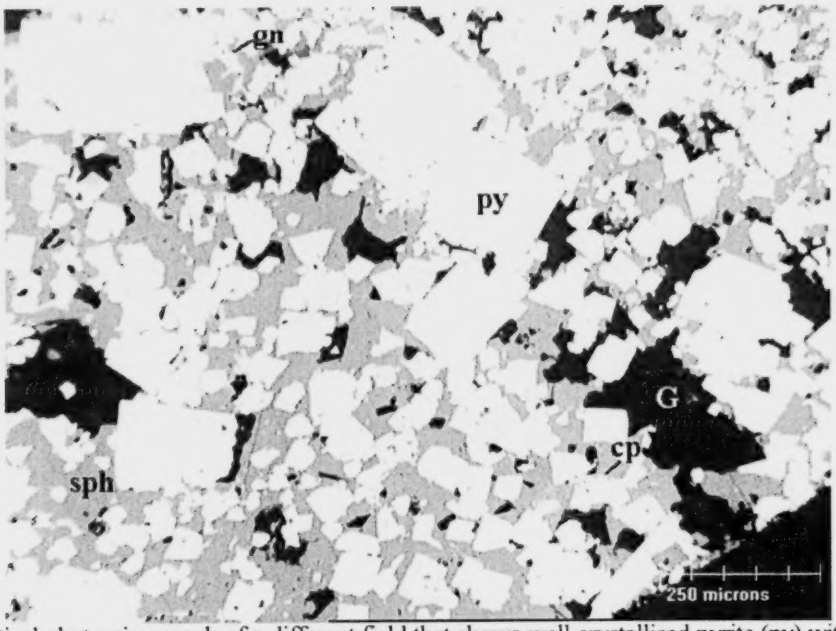

Figure 7. Optical photomicrograph of a different field that shows well crystallised pyrite (py) within a sphalerite-rich matrix (sph), with minor to trace amounts of galena (gn) and chalcopyrite (cp) and gangue (mainly quartz, G); Sample C

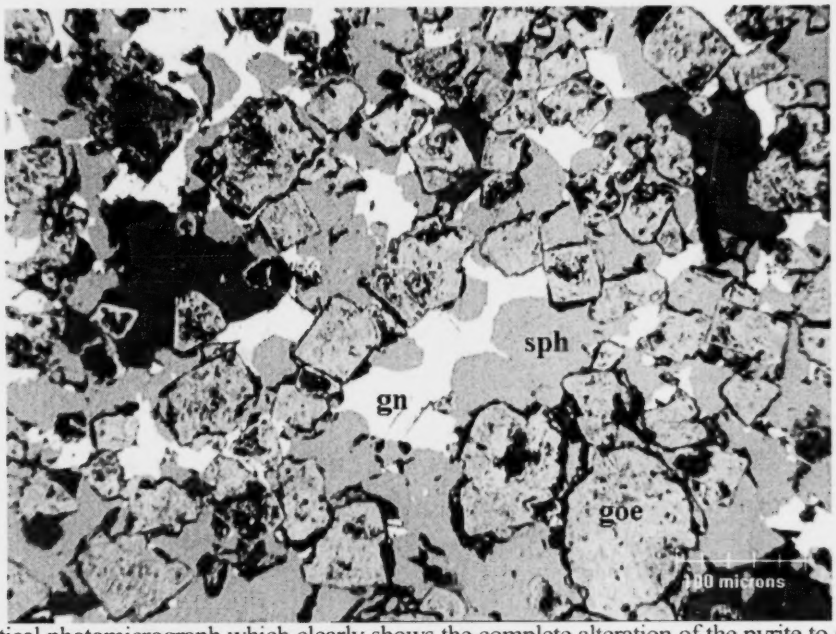

Figure 8. Optical photomicrograph which clearly shows the complete alteration of the pyrite to a goethite-like phase (goe) within a sphalerite-rich matrix (sph), with disseminated fine-grained galena (gn); Sample C-M

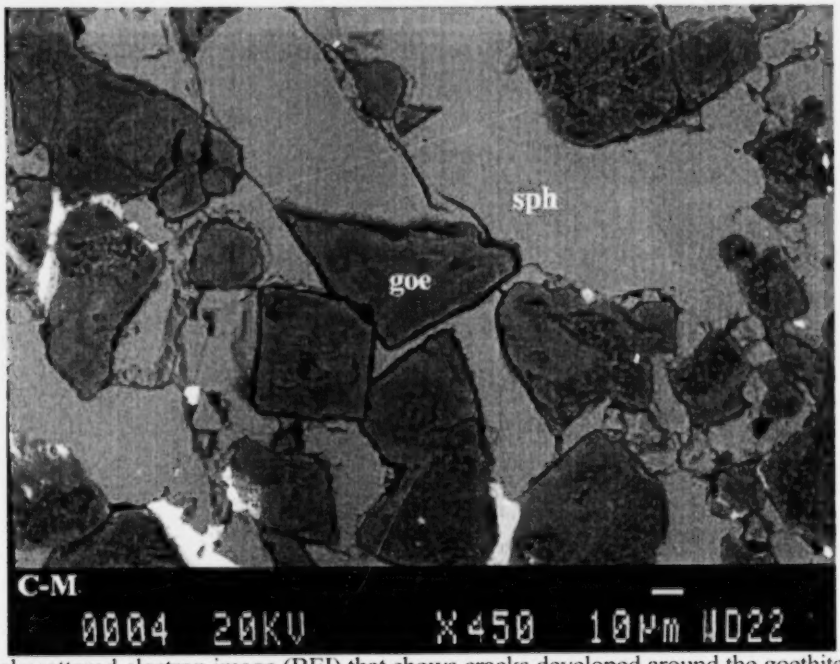

Figure 9. Backscattered electron image (BEI) that shows cracks developed around the goethite-like (goe) grains, within a sphalerite-rich matrix (sph); Sample C-M

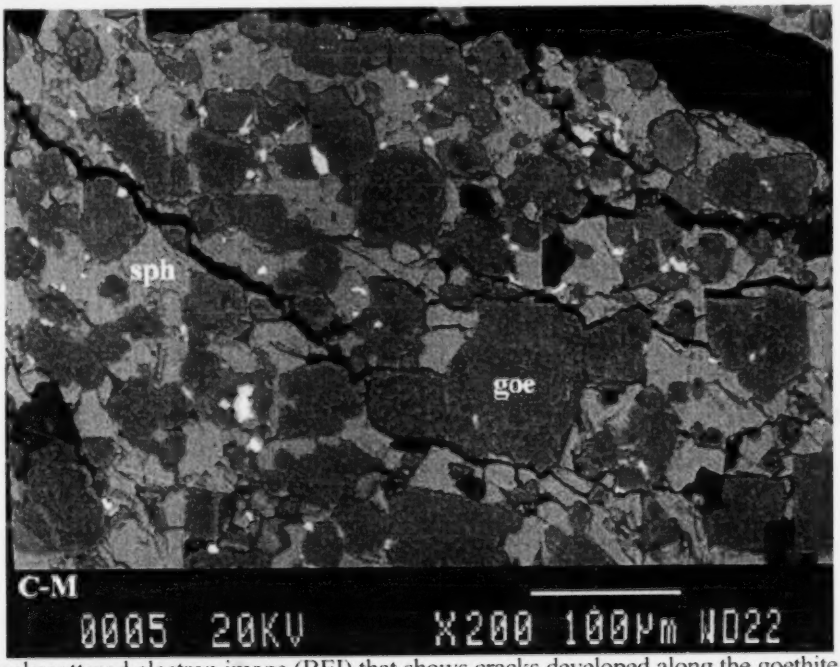

Figure 10. Backscattered electron image (BEI) that shows cracks developed along the goethite (goe) grain boundaries but also across the sphalerite (sph) matrix; Sample C-M

Figure 7. Optical photomicrograph of a different field that shows well crystallised pyrite (py) within a sphalerite-rich matrix (sph), with minor to trace amounts of galena (gn) and chalcopyrite (cp) and gangue (mainly quartz, G); Sample C

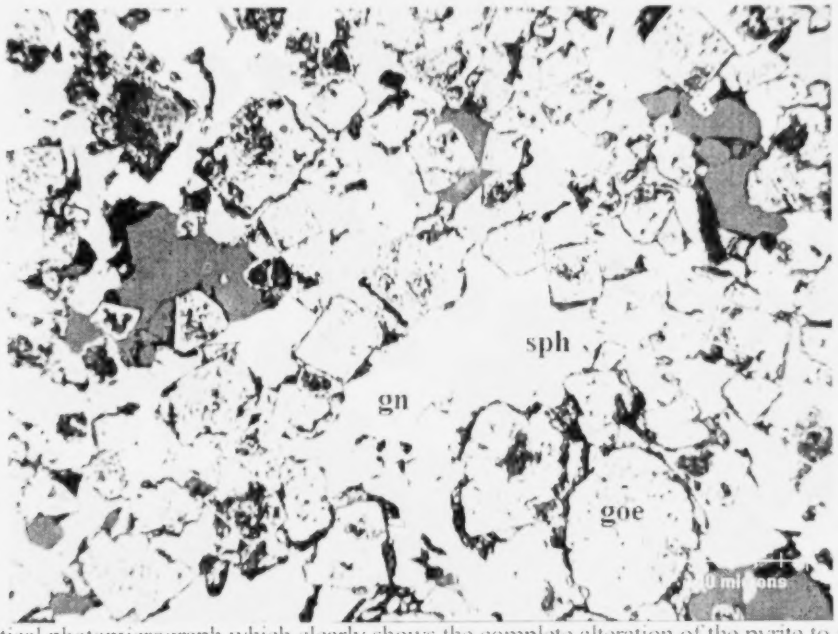

Figure 8. Optical photomicrograph which clearly shows the complete alteration of the pyrite to a goethite-like phase (goe) within a sphalerite-rich matrix (sph), with disseminated fine-grained galena (gn); Sample C-M

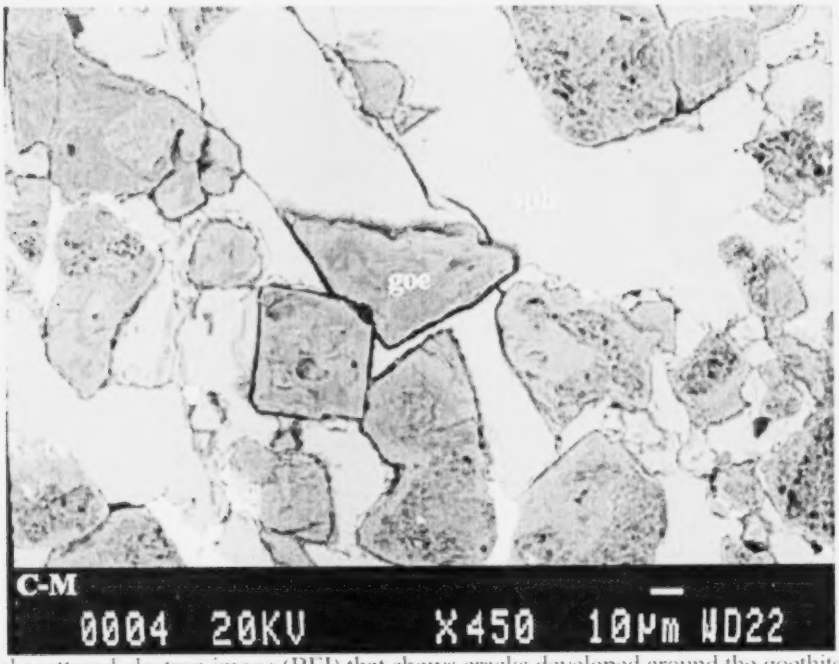

Figure 9. Backscattered electron image (BEI) that shows cracks developed around the goethite-like (goe) grains, within a sphalerite-rich matrix (sph); Sample C-M

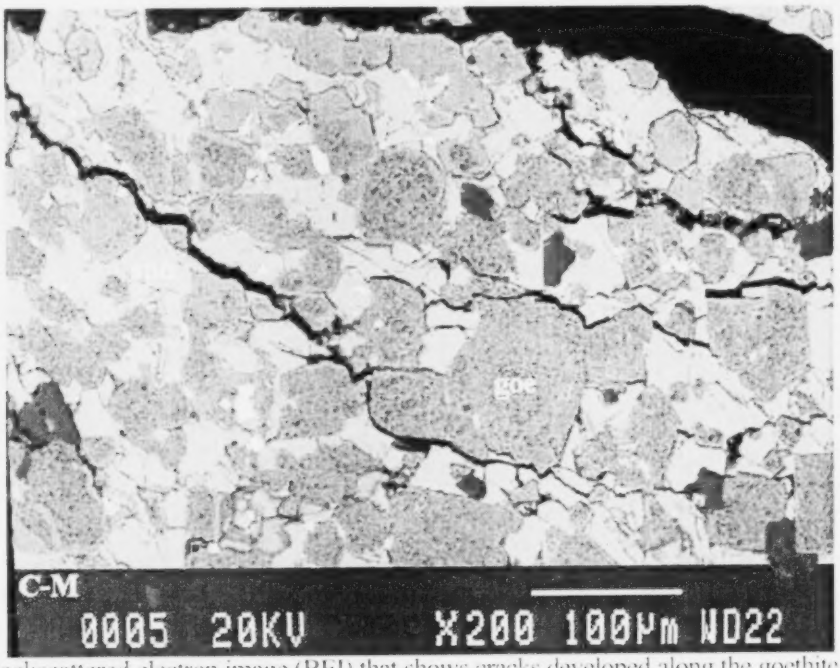

Figure 10. Backscattered electron image (BEI) that shows cracks developed along the goethite (goe) grain boundaries but also across the sphalerite (sph) matrix; Sample C-M